Annals of Operations Research (2023) 326:537–560
https://doi.org/10.1007/s10479-023-05302-9

ORIGINAL - OR MODELING/CASE STUDY

Analysing the benefits of trajectory deviations for planar trajectory optimisation

Salman Arif[1] · **Jason Atkin**[1] · **Geert De Maere**[1]

Accepted: 17 March 2023 / Published online: 19 April 2023

Abstract
Aircraft traverse airspace sectors under the supervision of Air Traffic Controllers by following navigation points. The trajectories can deviate from these points under the supervision of controllers. However, the controllers have to consider various factors for managing air traffic which increases their workload. We aim to offline analyse the potential benefits of trajectory deviations, by tactically shifting navigation points for planar trajectory optimisation of multiple aircraft at an enroute sector level. Historic deviations of trajectories are considered for this analysis to implement them at practical level. Within nominal speed and turning rate of aircraft trajectories, 5.47% reduction in time cost and an annual fuel saving worth US$ 29.32 million has been estimated using shifts for an airspace sector.

Keywords Air tyraffic flow management · Trajectory deviations · Navigation points · Trajectory optimisation · Air Traffic Controllers

1 Introduction

The enroute airspace is divided into various sectors, each one having entry and exit points by which the aircraft enter and leave the sectors, and waypoints by following which the aircraft traverse the airspace in these sectors (Kistan et al., 2017; Flener et al., 2007). These navigation points are located on airways that are similar to highways on the ground, by following which the aircraft complete their traversal along routes determined by the airlines (Gurtner et al., 2017; Clarke et al., 1997). However, the delay in flights in enroute airspace has been majorly contributing to the overall (Air Traffic Flow Management) ATFM delay for

This work was supported by the University of Nottingham.

✉ Salman Arif
salman.arif@nottingham.ac.uk

Jason Atkin
jason.atkin@nottingham.ac.uk

Geert De Maere
geert.demaere@nottingham.ac.uk

[1] School of Computer Science, University of Nottingham, Jubilee Campus, Wollaton Road, Nottingham, UK

last ten years due to the shortage in the enroute airspace capacity (Eurocontrol, 2020, 2018). In order to improve the airspace capacity and safety for air traffic, next generation systems considered by NextGen in the US and SESAR (Single European Sky ATM Research) in Europe have planned the automated trajectory optimisation to be a key component for the improved decision making by the Air Traffic Controllers (ATCs) (Schuster & Ochieng, 2014; Planning, 2008; SESAR, 2007).

Aircraft Trajectory Optimisation is mainly focussed on optimising the aircraft trajectories by reducing their direct operational costs (fuel and time costs), resolving conflicts among them and enabling easy manoeuvres during their traversal. It is a multi-objective problem with multiple stakeholders (Yang et al., 2017). The pilots prefer easy manoeuvres for routing the aircraft without intense speed changes or sharp turns while the airlines aim to maximise their revenue by saving fuel and time costs (Cook et al., 2009). On the other hand, the ATCs are responsible for the safety and regulation of air traffic within their respective sectors (Barnier & Brisset, 2004), and consider multiple factors that can impact the complexity of air traffic situation (Ren & Li, 2018; Flener et al., 2007), like airway structure, positions of entry, exit and waypoints, the number of aircraft, speed and heading of the air traffic. This makes it difficult for the ATCs to manually optimise the aircraft trajectories in air traffic situations due to high complexity.

This paper provides an offline analysis of the potential benefits of trajectory deviations, by tactically (i.e. at flying time, when information is available about other aircraft) shifting the positions of navigation points for automated trajectory optimisation of multiple aircraft at a planar (2D) level in an enroute sector. A Mixed Integer Linear Programming (MILP) model has been formulated for analysing the benefits by extending the model given in Richards and How (2002). The proposed model is also a step forward towards automation for trajectory optimisation as it offers benefits for the aforementioned stakeholders; by formulating the basic ATC activities for rerouting trajectories across the sector; by focussing on minimisation of direct operational costs for the benefit of airlines; and by restricting intense speed changes and sharp turns to ease manoeuvring for the pilots. It will be seen in Sect. 5 that these benefits are estimated to save fuel and reduce time cost for trajectories.

Following the problem description and literature review in Sect. 2, an analysis has been conducted in Sect. 3 for finding the real world deviations of aircraft trajectories from the route centreline, to make the implemented deviations by the model manageable in practice for the ATCs. This section also elaborates a side analysis for estimating the aircraft trajectories that traverse at a constant flight level (planar level) in historic real world data, for signifying the importance of planar trajectory optimisation. The proposed model is then formulated in Sect. 4 and validated against scenarios based on the real world airway structure and operational air traffic data in Sect. 5.

2 Problem description and previous work

The traversal through an airspace sector takes place in three phases. The aircraft in the first phase enters the sector through an assigned entry point, traverses through the sector during the second phase by visiting its defined series of waypoints and leaves the sector through an assigned exit point in the final phase. For conflict avoidance, the aircraft is bounded by a cylindrical safety region with radius of 5 nautical miles (NM) (Chaimatanan et al., 2015) To regulate the flow of air traffic and resolve conflicts among the aircraft trajectories, the ATCs implement trajectory based operations by rerouting, changes in speed or flight level

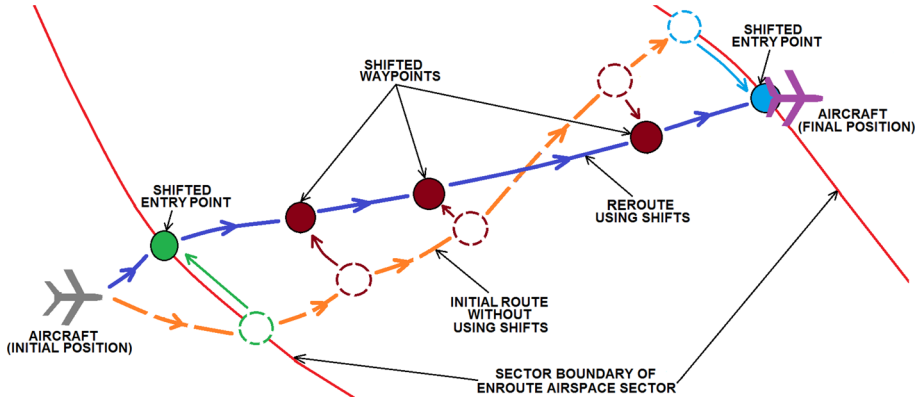

Fig. 1 Planar rerouting of aircraft trajectory using shifts in navigation points, compared to initial route without using shifts in an enroute airspace sector. (Color figure online)

(Alonso-Ayuso et al., 2014) The first two manoeuvres are implemented at constant flight level for planar (2D) trajectory optimisation, which makes it common in Air Traffic Management (ATM) models as the enroute airspace is vertically stratified in layers of flight levels (Richards & How, 2002) The third manoeuvre extends the problem at 3D level for spatial trajectory optimisation, and is more likely to perturb passenger comfort level as compared to the first two manoeuvres due to change in flight levels (Frazzoli et al., 2001)

The pilots during traversal through the sector may ask the ATCs to allow deviation from the route centreline or vice versa, the ATCs may direct them to do so for various reasons (Carreras-Maide et al., 2020) We assume this problem at planar level by fixing the flight levels for the trajectories and modelling safety region around them to be circular. A planar trajectory in a straight line with reduced travelling distance, obtained by changing its initial route using the shifts during its traversal through an enroute airspace sector is shown in Fig. 1

The literature on trajectory optimisation can be categorised based upon the scope of its application. The studies focussed on optimisation of an individual aircraft trajectory can be classified under Trajectory Planning, which is focussed on the reduction of direct operational costs, noise, gas emission and contrail formation. However, the studies focussed on optimising multiple trajectories have a common feature of simultaneously resolving conflicts among those trajectories and can be grouped under Trajectory Deconfliction.

Murrieta Mendoza and Botez (2014) aim to reduce the direct operational costs in climb and descent for a trajectory while Soler et al. (2014) aim to manage the trade-off between fuel consumption and contrail formation for trajectories at an individual level. However,

Adacher et al. (2017) implement rerouting at inter-sector level by forming a network of aircraft trajectories and, Richards and How (2002) use rerouting with fixed waypoints while keeping speed constant at maximum. At 3D level, Chaimatanan et al. (2015) focus on spatial trajectory optimisation while considering uncertainty in the position of aircraft. Similarly, Vela et al. (2009) use speed changes and flight level assignments for conflict resolution.

Some studies highlight the importance of trajectory deviations. Bongiorno et al. (2017); Carreras-Maide et al. (2020) suggest that the aircraft trajectories in the real world are more likely to deviate from their planned path (i.e. route in their flight plan) by shifting from navigation points to reduce their length and direct operational costs. As per the ATCs, these deviations happen to allow aircraft to traverse in straight lines, as the airways constituting their route are not configured in straight lines. The routes in flight plans are not optimised but help

the flights to be predictable for the ATCs. This signifies the importance of the proposed work here. But, there are hardly any studies that focus on exploiting the positions of navigation points for trajectory deconfliction in spite of their impact on the complexity of air traffic situation, the number of potential conflicts and consequently the workload for ATCs (Hossain et al., 2014; Wang et al., 2018). For example, the complexity of air traffic situation can increase two folds when an aircraft approaches an entry or exit point from 20 Nautical Miles (NM) to 10NM (Delahaye & Puechmorel, 2000) Some studies, for example Chaimatanan et al. (2014, 2015), consider planar shifts in waypoints for strategically resolving conflicts among trajectories at continental level using metaheuristics like simulated annealing. Krozel et al. (2004, 2006) implement shifts in entry and exit points for synthesizing routes in weather constrained regions, using optimal path algorithms and dynamic programming. Similarly, Alam et al. (2015) consider optimising planar shifts of aircraft trajectories from oceanic entry points about 1-2 NM as per the Strategic Lateral Offset Procedure (SLOP), by using an evolutionary algorithm. However, Carreras-Maide et al. (2020) seems to be the only study as per its claim and also in our knowledge that analyses the impact of trajectory deviations on the financial costs of aircraft trajectories. This makes researchers less aware of the importance for trajectory deviations and explains why few studies considered shifting aircraft trajectories in optimisation.

Alternative approaches adopted by the aforementioned previous studies used metaheuristics for trajectory optimisation, that generally give a good solution but do not guarantee an optimal solution. However, dynamic programming has been commonly adopted by previous studies for deriving optimal control paths for aircraft trajectories. On the other hand, integer programming and MILP has been commonly used for optimising multiple aircraft trajectories by discretising space or time (Qian et al., 2017; Richards & How, 2002), and the proposed approach in this article also uses MILP which guarantees an optimal solution. Obtaining an optimal solution using MILP helps to accurately analyse the potential benefits of trajectory deviations, which is the main objective of this paper. In order to build a decision support system to implement real-time trajectory deviations for the ATCs, heuristics could be used as they give solution in less computation time as compared to using MILP.

The next section analyses the historic aircraft trajectory deviations based on the real world data, to implement deviations using the proposed model that are manageable in practice for the ATCs.

3 Finding historic deviations of aircraft trajectories from route centreline

144 Aircraft trajectories were studied from three major enroute sectors of UK airspace, Strumble, Daventry and Clacton, as shown in Fig. 2 during the timeline from March 2018 to February 2019. These airspace sectors cover most of London Flight Information Region (FIR) and, have different airspace characteristics like (airway structure, position of entry and exit points) and air traffic characteristics (like the load and heading of air traffic). Twelve aircraft trajectories were selected in each month. The root mean square (RMS) and maximum value of their deviations is shown in Fig. 3. These deviations have been calculated based on the distance of every individual trajectory from its closest airway.

Even by removing the case of outliers, many trajectories have been observed to show deviations of RMS value more than 2NM and the maximum value more than 5NM as shown in Fig. 4.

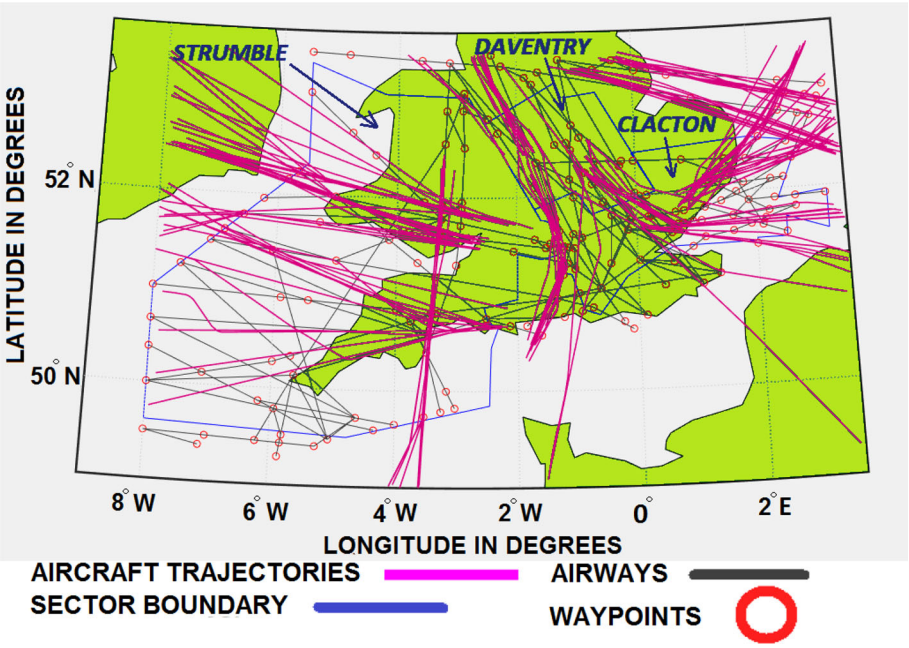

Fig. 2 Plots of aircraft trajectories used in our survey against real world airway structure in Strumble, Daventry and Clacton Airspace Sectors. (Color figure online)

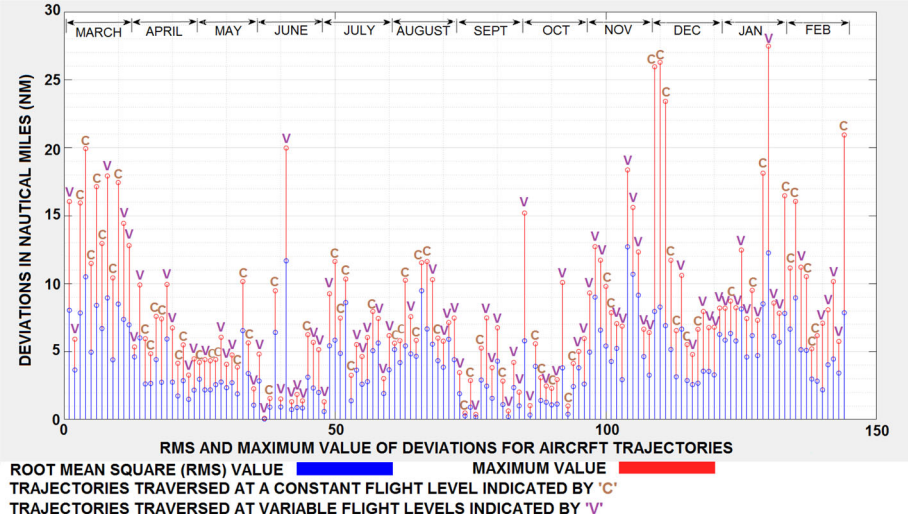

Fig. 3 Plots of RMS and maximum value for deviations of aircraft trajectories used in our analysis. (Color figure online)

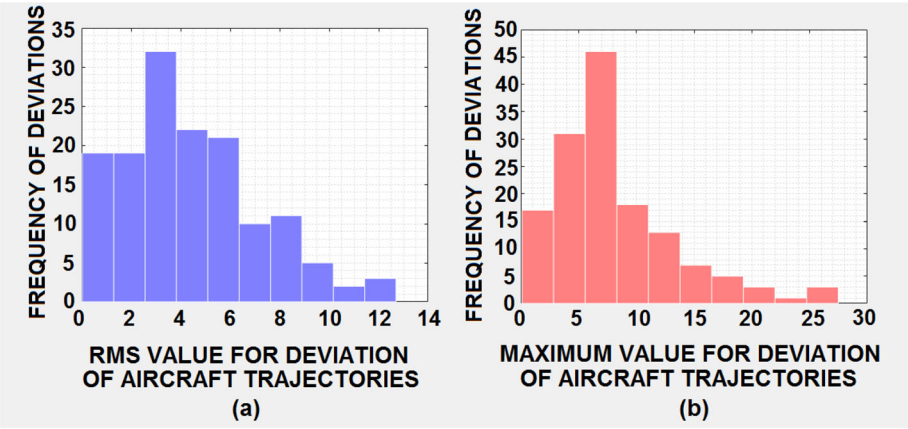

Fig. 4 Histogram for **a** RMS value and **b** maximum value of deviations for aircraft trajectories used in our survey. (Color figure online)

Furthermore, the largest maximum value of deviation has been found to be 27NM that is high in magnitude to occur from a route centreline. It has been observed in north-west region of Strumble where airways are relatively more distant from each other. Although as per the ATCs, it is noted and confirmed that larger trajectory deviations are possible under adverse weather conditions. Therefore, it is not unusual for the aircraft trajectories to deviate from the route centreline under the supervision of the ATCs, which indicates the significance of trajectory deviations.

Moreover, the aircraft trajectories that traversed at a constant flight level and those that traversed at variable flight levels in enroute airspace are also observed in Fig. 3, using the indicators C and V respectively. 43.1% of the trajectories have been found to traverse at a constant flight level which is a considerable amount as compared to the other set of trajectories.

4 Model formulation

This section introduces a multi-objective Mixed Integer Linear Programming (MILP) model for tactically rerouting aircraft trajectories at planar level, both with and without shifts in navigation points across an enroute airspace sector. The proposed model improves the previous models in limiting the turning rate of aircraft within its nominal value, and the speed within its nominal and minimum flyable value unlike Chaimatanan et al. (2014, 2015) that do not consider implementation of these limits. The model also implements order in visiting of navigation points across the sector and allows speed changes for trajectory rerouting unlike Richards and How (2002), that do not ensure order in visiting navigation points and only allows maximum turning rate but with constant speed and limited force. Moreover, the model formulates the safety region around aircraft more accurately than Richards and How (2002), who formulate the region in the form of a square. These improvements help in deriving trajectory solutions closer to real world conditions.

The time instances or steps for this model have been discretised. The proposed model begins with the formulation of dynamics of aircraft, followed by formulation of constraints for conflict avoidance and trajectory rerouting through shifted navigation points, ending up at the derivation of objective function.

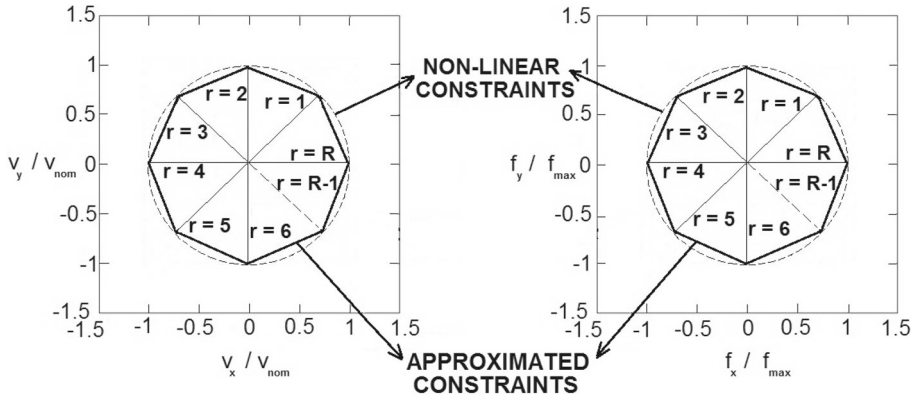

Fig. 5 Linear approximations for non-linear constraints of velocity and force

4.1 Discrete dynamics for aircraft

The discrete dynamics for aircraft are formulated by considering a total number of N_A aircraft, each having a point mass on a 2D plane, in a set of total T discrete time steps. Then, the constraints for position (x_{ip}, y_{ip}), velocity $(v_{x_{ip}}, v_{y_{ip}})$ and force i.e. acceleration $(f_{x_{ip}}, f_{y_{ip}})$, for aircraft p at an i^{th} time step are formulated in Eqs. (1) and (2) as follows.

$$\begin{aligned}
&\forall i \in [1 \dots T] \quad \forall p \in [1 \dots N_A] \\
&x_{(i+1)p} \leq x_{ip} + v_{x_{ip}} + M g_{ip} \\
&x_{(i+1)p} \geq x_{ip} + v_{x_{ip}} - M g_{ip} \\
&y_{(i+1)p} \leq y_{ip} + v_{y_{ip}} + M g_{ip} \\
&y_{(i+1)p} \geq y_{ip} + v_{y_{ip}} - M g_{ip}
\end{aligned} \tag{1}$$

$$\begin{aligned}
&\forall i \in [1 \dots T] \quad \forall p \in [1 \dots N_A] \\
&v_{x_{(i+1)p}} \leq v_{x_{ip}} + f_{x_{ip}} + M g_{ip} \\
&v_{x_{(i+1)p}} \geq v_{x_{ip}} + f_{x_{ip}} - M g_{ip} \\
&v_{y_{(i+1)p}} \leq v_{y_{ip}} + f_{y_{ip}} + M g_{ip} \\
&v_{y_{(i+1)p}} \geq v_{y_{ip}} + f_{y_{ip}} - M g_{ip}
\end{aligned} \tag{2}$$

where the boolean decision variable g_{ip} becomes 1 and relaxes the above formulated constraints as soon as the aircraft p visits its respective exit point using M, which has a value larger than any possible distance. This decision variable is defined in Eq. (20).

Moreover, the constraints on position for an aircraft p at an ith time step are given in Eq. (3). Velocity and force are modelled as two rectangular components for x and y. A simple calculation of absolute velocity and force using these components $\sqrt{x^2 + y^2}$ is not linear, so a series of R linear constraints are applied to ensure that the absolute velocity and force are kept below a specified limit. This is formulated below in Eqs. (4) and (5) from Richards and How (2002), as shown in Fig. 5.

$$\begin{aligned}
&\forall i \in [1 \dots T] \quad \forall p \in [1 \dots N_A] \\
&x_{min} \leq x_{ip} \leq x_{max}
\end{aligned} \tag{3}$$

$$\text{and} \quad y_{min} \le y_{ip} \le y_{max}$$
$$\forall i \in [1 \dots T] \quad \forall p \in [1 \dots N_A] \quad \forall r \in [1 \dots R]$$
$$v_{x_{ip}} \sin\left(\frac{2\pi r}{R}\right) + v_{y_{ip}} \cos\left(\frac{2\pi r}{R}\right) \le v_{nom}(1 - g_{ip}) \tag{4}$$
$$\forall i \in [1 \dots T] \quad \forall p \in [1 \dots N_A] \quad \forall r \in [1 \dots R]$$
$$f_{x_{ip}} \sin\left(\frac{2\pi r}{R}\right) + f_{y_{ip}} \cos\left(\frac{2\pi r}{R}\right) \le f_{max}(1 - g_{ip}) \tag{5}$$

Where Eq. (3) defines limits on the position of aircraft p, the constraints in Eq. (4) restrict the velocity components for aircraft p from exceeding its nominal (usual) speed v_{nom} during all i time steps and, the constraints in Eq. (5) restrict the magnitude of force components from exceeding their maximum value f_{max}. However, g_{ip} relaxes these constraints once aircraft leaves the sector, so that the velocity and force contribute zero value to the objective function in Eq. (26).

The constraints for minimum flyable speed v_{min_fly} and nominal turning rate w_{nom} are formulated similar to Eqs. (4) and 5. The aircraft p is restricted to remain above the limit of v_{min_fly}, that is required to maintain flight at a constant flight level using Eq. (6). Similar to Richards and How (2002), the force in Eq. (5) at i^{th} time step is required to turn aircraft p having mass m_p travelling with velocity in Eq. (4) within the limit of w_{nom} as given in Eq. (7).

$$\forall i \in [1 \dots T] \quad \forall p \in [1 \dots N_A] \quad \forall r \in [1 \dots R]$$
$$v_{x_{ip}} \sin\left(\frac{2\pi r}{R}\right) + v_{y_{ip}} \cos\left(\frac{2\pi r}{R}\right) \ge v_{min\_fly} - Mg_{ip} \tag{6}$$
$$\forall i \in [1 \dots T] \quad \forall p \in [1 \dots N_A] \quad \forall r \in [1 \dots R]$$
$$\omega_{nom} \ge \frac{f_{x_{ip}} \sin\left(\frac{2\pi r}{R}\right) + f_{y_{ip}} \cos\left(\frac{2\pi r}{R}\right)}{m_p \left[v_{x_{ip}} \sin\left(\frac{2\pi r}{R}\right) + v_{y_{ip}} \cos\left(\frac{2\pi r}{R}\right)\right]} - Mg_{ip} \tag{7}$$

where w_{nom} equals 3°/s for all aircraft trajectories (Archibald et al., 2008) and the R constraints are formulated separately for both velocity and force. It is to be noted that restricting velocity and turning rate for aircraft trajectories within their nominal value prevents intense speed changes and sharp turns, which consequently enables easy manoeuvres favouring the pilots.

4.2 Conflict avoidance constraints

The constraints for circular safety region around the aircraft are formulated by considering the constraints on velocity in Eq. (4) and force in Eq. (5). Following the same notation as in Sect. 4.1, a conflict between aircraft p having position (x_{ip}, y_{ip}) and aircraft q having position (x_{iq}, y_{iq}) will be avoided at i^{th} time step if the distance between these two aircraft is greater than or equal to the radius of safety region s_{min}, which is shown in Fig. 6and formulated as follows in Eq. (8):

$$\forall i \in [1 \dots T] \quad \forall p, q \in [1 \dots N_A] \quad \forall r \in [1 \dots R]$$
$$|x_{ip} - x_{iq}| \sin\left(\frac{2\pi r}{R}\right) + |y_{ip} - y_{iq}| \cos\left(\frac{2\pi r}{R}\right) \ge s_{min} - Mg_{ip} - Mg_{iq} \tag{8}$$

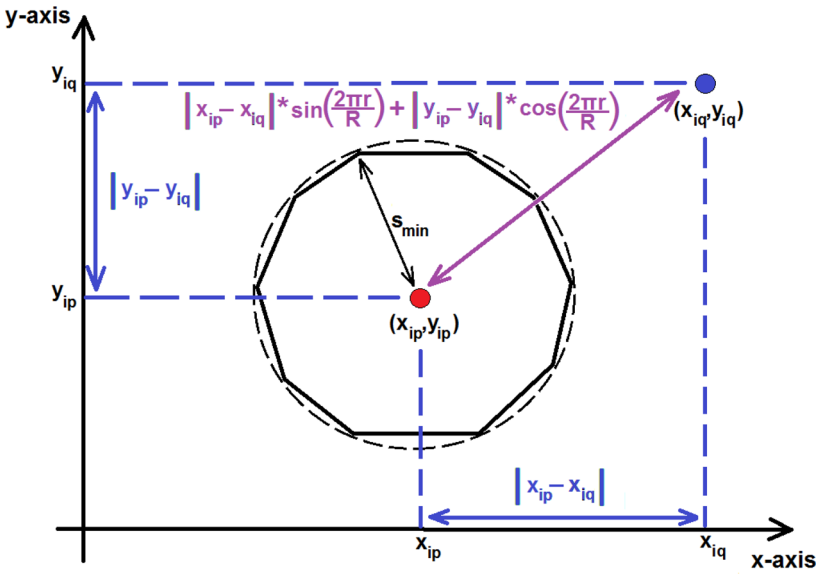

Fig. 6 Conflict avoidance between the aircraft p and q. (Color figure online)

4.3 Trajectory rerouting through shifted navigation points

The constraints for rerouting aircraft trajectories through shifted navigation points across the sector are formulated based on the formulation in Richards and How (2002) for rerouting an aircraft towards its destination. These constraints also represent basic ATC activities for trajectory rerouting i.e. assignment of entry and exit points, and rerouting through navigation points.

By following the same notation in Sect. 4.1, an aircraft p is rerouted to its required destination (x_{dp}, y_{dp}) as formulated below in Eq. (9) and Eq. (10):

$$\begin{aligned} \forall i \in [1 \ldots T] \quad \forall p \in [1 \ldots N_A] \\ x_{ip} - x_{dp} \;&\leq\; M(1 - b_{ip}) \\ x_{ip} - x_{dp} \;&\geq\; -M(1 - b_{ip}) \\ y_{ip} - y_{dp} \;&\leq\; M(1 - b_{ip}) \\ y_{ip} - y_{dp} \;&\geq\; -M(1 - b_{ip}) \end{aligned} \tag{9}$$

$$\forall p \in [1 \ldots N_A] \quad \sum_{i=1}^{T} b_{ip} \;=\; 1 \tag{10}$$

where the boolean decision variable $b_{ip} = 1$ means that the aircraft p is required to reach its destination at the i^{th} step and $b_{ip} = 0$ relaxes the constraints in Eq. (9). By doing so, this decision variable decides the choice of time step at which the aircraft reaches its destination through Eq. (10), which forces b_{ip} to become 1 at any ith time step from the set of all time steps. Using these constraints, the aircraft is required to visit its destination only once, which also applies for visiting waypoints, entry and exit points.

4.3.1 Phase 1 and 3: assignment and rerouting for shifted entry and exit points

The sector boundaries are polygon shaped, while the entry and exit points are located at the vertices or sides (edges) of these linear boundaries. For rerouting the aircraft trajectories through entry points, the constraints in Eqs. (9) and (10) are extended by assuming N_{en_p} number of entry points located on a sector boundary that are in proximity to the trajectory of aircraft p. The assignment of an entry point l and rerouting of the aircraft p to that entry point's location $(x_{en_{lp}}, y_{en_{lp}})$ required to be completed by a certain time step T_{en_p} is formulated in Eq. 11, 12 and 13 as follows:

$$\begin{aligned}
&\forall i \in [1 \dots T_{en_p}] \quad \forall p \in [1 \dots N_A] \quad \forall l \in [1 \dots N_{en_p}] \\
&x_{ip} - x_{en_{lp}} \leq M(1 - b_{en_{ip}}) + M(1 - c_{lp}) \\
&x_{ip} - x_{en_{lp}} \geq -M(1 - b_{en_{ip}}) - M(1 - c_{lp}) \\
&y_{ip} - y_{en_{lp}} \leq M(1 - b_{en_{ip}}) + M(1 - c_{lp}) \\
&y_{ip} - y_{en_{lp}} \geq -M(1 - b_{en_{ip}}) - M(1 - c_{lp})
\end{aligned} \tag{11}$$

$$\forall p \in [1 \dots N_A] \quad \sum_{i=1}^{T_{en_p}} b_{en_{ip}} = 1 \tag{12}$$

$$\forall p \in [1 \dots N_A] \quad \sum_{l=1}^{N_{en_p}} c_{lp} = 1 \tag{13}$$

where the boolean decision variable $b_{en_{ip}} = 1$ decides the choice of i^{th} time step at which the aircraft has to visit an entry point. Similarly, the boolean decision variable c_{lp} decides the assignment of entry point l to the aircraft p.

Now, implementation of shifts in the entry points are considered as given in Fig. 7a. These points can be linearly shifted on either side of the boundary so that their coordinates follow the line denoting the side of the sector boundary. Each side can be defined by a linear equation using slope-intercept formula for shifting entry points within a certain range of parameters, while considering entry points as reference points for shifts. An entry point l from a set of N_{en_p} number of entry points in proximity to the aircraft p is shifted along x-axis by $x_{en\_shift_{lp}}$ and along y-axis by $y_{en\_shift_{lp}}$ on either side of the sector boundary, using slope $m_{en\_slope(1)_{lp}}$ for $Side\,1$ or $m_{en\_slope(2)_{lp}}$ for $Side\,2$ respectively. This is shown in Fig. 7a and formulated in Eq. (14) as follows.

$$\begin{aligned}
&\forall p \in [1 \dots N_A] \quad \forall l \in [1 \dots N_{en_p}] \\
&x_{en_min(1)_{lp}} \leq x_{en_shift_{lp}} \leq x_{en_max(1)_{lp}} \\
&y_{en_min(1)_{lp}} \leq y_{en_shift_{lp}} \leq y_{en_max(1)_{lp}} \\
&y_{en_shift_{lp}} = m_{en_slope(1)_{lp}} x_{en_shift_{lp}} \\
&\text{OR} \\
&x_{en_min(2)_{lp}} \leq x_{en_shift_{lp}} \leq x_{en_max(2)_{lp}} \\
&y_{en_min(2)_{lp}} \leq y_{en_shift_{lp}} \leq y_{en_max(2)_{lp}} \\
&y_{en_shift_{lp}} = m_{en_slope(2)_{lp}} x_{en_shift_{lp}}
\end{aligned} \tag{14}$$

where $x_{en\_max(1)_{lp}}$ and $x_{en\_min(1)_{lp}}$ are the parameters defining maximum and minimum limits for shift along x-axis $x_{en\_shift_{lp}}$ on $Side\,1$ and, $y_{en\_max(1)_{lp}}$ and $y_{en\_min(1)_{lp}}$ define

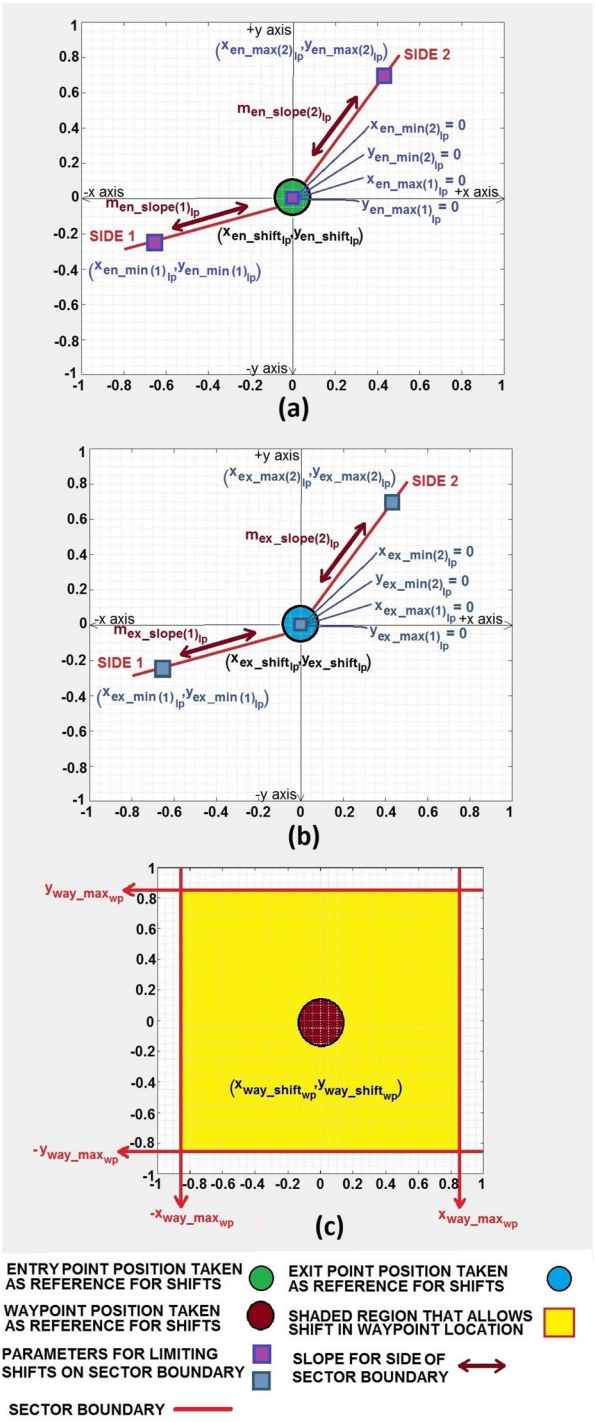

Fig. 7 Shifting **a** entry points, **b** exit points and **c** waypoints using planar shifts. (Color figure online)

maximum and minimum limits for shift along y-axis $y_{en\_shift_{lp}}$ on the same side. Similarly, $x_{en\_max(2)_{lp}}$, $x_{en\_min(2)_{lp}}$, $y_{en\_max(2)_{lp}}$, $y_{en\_min(2)_{lp}}$, are the parameters that define range for these shifts on $Side\,2$. All these parameters are constants that limit variable shifts $x_{en\_shift_{lp}}$ and $y_{en\_shift_{lp}}$ on each side of the sector boundary, considering shifts happen only on one side of the boundary individually for each aircraft, either on $Side\,1$ or on $Side\,2$.

The above formulation allows entry points to shift on the sector boundary within a certain range of units (for example Nautical Miles) and analyse the impact on rerouting these trajectories by varying the limitation for shifts. Now the constraints for rerouting aircraft trajectories through assigned entry points in Eq. (11) are reformulated using the shifts for entry points derived in Eq. (14) as follows in Eq. (15).

$$\begin{aligned} &\forall i \in [1 \ldots T_{en_p}] \quad \forall p \in [1 \ldots N_A] \quad \forall l \in [1 \ldots N_{en_p}] \\ x_{ip} - (x_{en_{lp}} + x_{en\_shift_{lp}}) &\leq \quad M(1 - b_{en_{ip}}) \; + M(1 - c_{lp}) \\ x_{ip} - (x_{en_{lp}} + x_{en\_shift_{lp}}) &\geq -M(1 - b_{en_{ip}}) - M(1 - c_{lp}) \\ y_{ip} - (y_{en_{lp}} + y_{en\_shift_{lp}}) &\leq \quad M(1 - b_{en_{ip}}) + M(1 - c_{lp}) \\ y_{ip} - (y_{en_{lp}} + y_{en\_shift_{lp}}) &\geq -M(1 - b_{en_{ip}}) - M(1 - c_{lp}) \end{aligned} \tag{15}$$

The exit points as shown in Fig. 7b serve as entry points by allowing the aircraft to enter another airspace sector by exiting from their current airspace sector. Therefore, the constraints for rerouting the aircraft trajectories through shifted exit points can be derived similarly to the above formulated constraints for rerouting the trajectories through shifted entry points.

An exit point n having position $(x_{ex_{np}}, y_{ex_{np}})$ assigned to aircraft p is shifted along slope $m_{ex\_slope(1)_{np}}$ for $Side\,1$ or $m_{ex\_slope(2)_{np}}$ for $Side\,2$ of the sector boundary, using shifts $x_{ex\_shift_{np}}$ $y_{ex\_shift_{np}}$ in the following Eq. (16) as shown in Fig. 7b:

$$\begin{aligned} &\forall p \in [1 \ldots N_A] \quad \forall n \in [1 \ldots N_{ex_p}] \\ &x_{ex\_min(1)_{np}} \leq x_{ex\_shift_{np}} \leq x_{ex\_max(1)_{np}} \\ &y_{ex\_min(1)_{np}} \leq y_{ex\_shift_{np}} \leq y_{ex\_max(1)_{np}} \\ &y_{ex\_shift_{np}} = m_{ex\_slope(1)_{np}} x_{ex\_shift_{np}} \\ &\qquad\qquad \text{OR} \\ &x_{ex\_min(2)_{np}} \leq x_{ex\_shift_{np}} \leq x_{ex\_max(2)_{np}} \\ &y_{ex\_min(2)_{np}} \leq y_{ex\_shift_{np}} \leq y_{ex\_max(2)_{np}} \\ &y_{ex\_shift_{np}} = m_{ex\_slope(2)_{np}} x_{ex\_shift_{np}} \end{aligned} \tag{16}$$

Using Eq. (16), the constraints for rerouting aircraft trajectories from their last waypoints towards shifted exit points are formulated as follows in Eq. (17), by considering an aircraft p required to visit an exit point n by time step T_{ex_p}:

$$\begin{aligned} &\forall p \in [1 \ldots N_A] \quad \forall n \in [1 \ldots N_{ex_p}] \\ &\forall i \in [T_{W_p} \ldots T_{ex_p} \mid T_{ex_p} \leq T] \\ x_{ip} - (x_{ex_{np}} + x_{ex\_shift_{np}}) &\leq \quad M(1 - b_{ex_{ip}}) + M(1 - d_{np}) \\ x_{ip} - (x_{ex_{np}} + x_{ex\_shift_{np}}) &\geq -M(1 - b_{ex_{ip}}) - M(1 - d_{np}) \\ y_{ip} - (y_{ex_{np}} + y_{ex\_shift_{np}}) &\leq \quad M(1 - b_{ex_{ip}}) + M(1 - d_{np}) \\ y_{ip} - (y_{ex_{np}} + y_{ex\_shift_{np}}) &\geq -M(1 - b_{ex_{ip}}) - M(1 - d_{np}) \end{aligned} \tag{17}$$

$$\forall p \in [1 \dots N_A] \quad \sum_{i=T_{W_p}}^{T_{ex_p}} b_{ex_{ip}} \; = \; 1 \tag{18}$$

$$\forall p \in [1 \dots N_A] \quad \sum_{n=1}^{N_{ex_p}} d_{np} \; = \; 1 \tag{19}$$

where T represents the largest time step, T_{W_p} represents time step by which aircraft visited its last waypoint W_p and N_{ex_p} represents the number of exit points close to the aircraft at the sector boundary. Moreover, $b_{ex_{ip}}$ in Eq. (18) decides the time step for aircraft p to reach exit point n in the time window between time steps T_{W_p} and T_{ex_p}, and d_{np} in Eq. (19) decides the choice for assignment of exit point to aircraft p. The boolean variable g_{ip} for relaxing the constraints in Sect. 4.1 and 4.2 is derived as follows in Eq. (20) using $b_{ex_{ip}}$:

$$\forall p \in [1 \dots N_A] \;\; \forall i \in [1 \dots T] \;\; g_{(i+1)p} = g_{ip} + b_{ex_{ip}} \tag{20}$$

where $b_{ex_{ip}}$ becomes 1 as the aircraft leaves the airspace sector and activates g_{ip} to relax the constraints for the rest of i time steps.

4.3.2 Phase 2: rerouting through shifted waypoints

Consider an aircraft p required to reach a waypoint w with location (x_{w_p}, y_{w_p}) within the time interval between time steps $T_{(w-1)_p}$ and T_{w_p}. Then, the constraints for rerouting aircraft p for total W_p number of waypoints are formulated in Eqs. (21) and (22) as follows:

$$\begin{aligned}
&\forall p \in [1 \dots N_A] \, \forall w \in [1 \dots W_p] \\
&\forall i \in [T_{(w-1)_p} \dots T_{w_p} \;\big|\; T_{(0)_p} = T_{en_p}] \\
&x_{ip} - x_{w_p} \;\leq\; M(1 - b_{way_{w_{ip}}}) \\
&x_{ip} - x_{w_p} \;\geq\; -M(1 - b_{way_{w_{ip}}}) \\
&y_{ip} - y_{w_p} \;\leq\; M(1 - b_{way_{w_{ip}}}) \\
&y_{ip} - y_{w_p} \;\geq\; -M(1 - b_{way_{w_{ip}}}) \quad \forall p \in [1 \dots N_A] \forall w \in [1 \dots W_p]
\end{aligned} \tag{21}$$

$$\sum_{i=T_{(w-1)p}}^{T_{w_p}} b_{way_{w_{ip}}} \; = \; 1 \tag{22}$$

where T_{w_p} is the time step by which aircraft p has to reach the waypoint w and $T_{(w-1)_p}$ is the time step by which this aircraft had visited the previous waypoint, given $T_{(w-1)_p} = T_{en_p}$ when the aircraft begins its traversal for first waypoint $w = 1$ after already visiting the entry point by T_{en_p}. By forcing every aircraft p to visit its waypoint w during the time window between T_{w_p} and $T_{(w-1)_p}$ as given in Eq. (21), each aircraft is restricted to visit waypoints in order of the time steps associated with them. Moreover, $b_{way_{w_{ip}}}$ decides the choice of i^{th} time step in the time window between T_{w_p} and $T_{(w-1)_p}$ at which the aircraft has to visit the waypoint w.

For shifting the waypoints, it must be noted that these points unlike entry and exit points are not located on the sector boundary, and therefore can be shifted in any direction within a certain region inside the sector airspace. This region can be specified by a certain set of parameters as shown in Fig. 7c. Considering a waypoint w for aircraft p in a 2 D plane to be the reference point for shift along x-axis $x_{way\_shift_{wp}}$ and shift along y-axis $y_{way\_shift_{wp}}$ in

its original position (x_{w_p}, y_{w_p}) taken as reference, then these shifts within their respective limits are formulated as follows in Eq. (23):

$$\begin{aligned} &\forall p \in [1 \dots N_A] \quad \forall w \in [1 \dots W_p] \\ &|x_{way\_shift_{wp}}| \leq |x_{way\_max_{wp}}| \\ &|y_{way\_shift_{wp}}| \leq |y_{way\_max_{wp}}| \end{aligned} \tag{23}$$

where $|x_{way\_max_{wp}}|$ limits $x_{way\_shift_{wp}}$ on x-axis between two extremes $x_{way\_max_{wp}}$ and $-x_{way\_max_{wp}}$ while $|y_{way\_max_{wp}}|$ restricts $y_{way\_shift_{wp}}$ between upper bound $y_{way\_max_{wp}}$ and lower bound $-y_{way\_max_{wp}}$ on y-axis as shown in Fig. 7c. These parameters help us to shift waypoint from its original position within a certain range of units (like Nautical Miles) and analyse the impact of varying shifts on aircraft trajectories.

By using the formulated shifts for waypoints in Eq. (23), the constraints for rerouting aircraft trajectories through a series of waypoints in Eq. (21) are reformulated to reroute the trajectories through a series of shifted waypoints as follows in Eq. (24):

$$\begin{aligned} &\forall w \in [1 \dots W_p] \ \forall p \in [1 \dots N_A] \\ &\forall i \in [T_{(w-1)_p} \dots T_{w_p} \mid T_{(0)p} = T_{en_p}] \\ x_{ip} - (x_{w_p} + x_{way\_shift_{wp}}) &\leq M(1 - b_{way_{w_{ip}}}) \\ x_{ip} - (x_{w_p} + x_{way\_shift_{wp}}) &\geq -M(1 - b_{way_{w_{ip}}}) \\ y_{ip} - (y_{w_p} + y_{way\_shift_{wp}}) &\leq M(1 - b_{way_{w_{ip}}}) \\ y_{ip} - (y_{w_p} + y_{way\_shift_{wp}}) &\geq -M(1 - b_{way_{w_{ip}}}) \end{aligned} \tag{24}$$

and Eq. (22) can now be used to decide the time step at which the reroute for the trajectories has to take place through shifted waypoints.

The overall rerouting of aircraft through an airspace sector by shifting entry points, waypoints and exit points based on the sequence of time steps is elaborated in Fig. 8.

4.4 Objective function

The airlines aim for revenue maximisation which can be contributed to by minimisation of fuel and time cost. The fuel cost of aircraft trajectories in the objective function is quantified in terms of their force (acceleration) and velocity cost. However, the time cost for every trajectory is calculated based on the time steps at which aircraft visit their navigation points, as given in Eq. (25). Here T_i is the actual value of time elapsed at an i^{th} time step and decision variables $b_{en_{ip}}$, $b_{way_{w_{ip}}}$ and $b_{ex_{ip}}$ indicate the time steps i at which aircraft p visits its entry point, waypoints and exit point respectively. By finding the total time cost, the velocity and force costs are incorporated in our objective function as follows in Eq. (26):

$$\begin{aligned} &\forall p \in [1 \dots N_A] \quad \forall i \in [1 \dots T] \\ &C_{T_{ip}} = T_i\left(b_{en_{ip}} + b_{way_{w_{ip}}} + b_{ex_{ip}}\right) \end{aligned} \tag{25}$$

$$\begin{aligned} \min J = \sum_{i=1}^{T} \sum_{p=1}^{N_A} \Big(&\alpha\, C_{T_{ip}} + \beta \left(|v_{x_{ip}}| + |v_{y_{ip}}|\right) \\ &+ \gamma \left(|f_{x_{ip}}| + |f_{y_{ip}}|\right) \Big) \end{aligned} \tag{26}$$

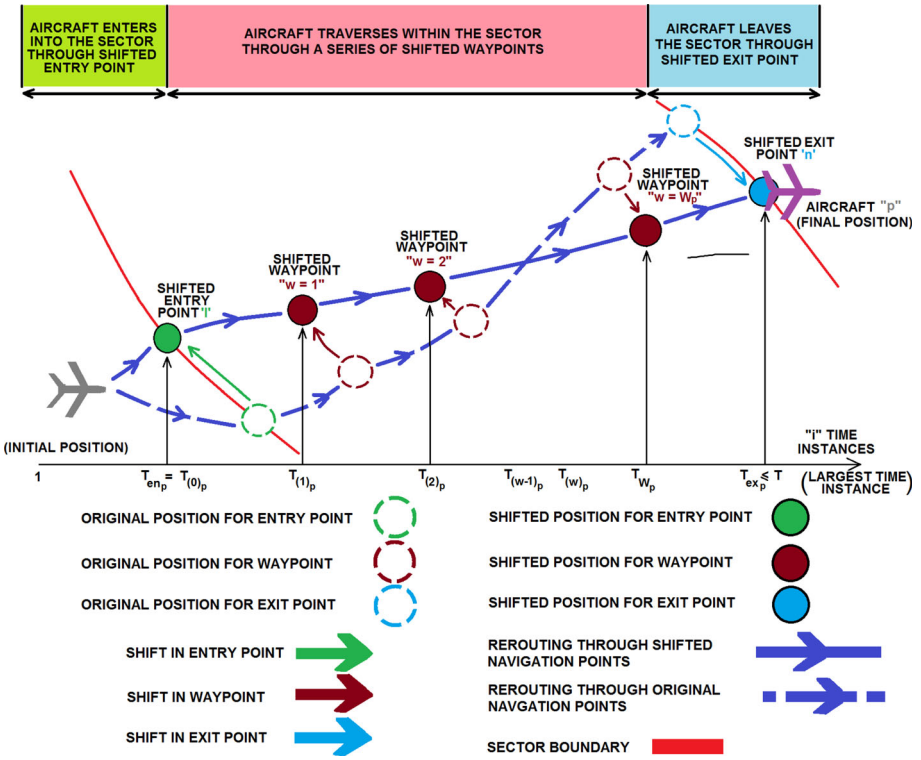

Fig. 8 An illustration of sector level rerouting of aircraft trajectory through shifted entry, exit and waypoints. (Color figure online)

where α, β and γ are the weights for time, velocity and force costs respectively. The value of these weights decides the priority for each cost and consequently affects the derived trajectory solutions. However, the objective function in Richards and How (2002) ignores cost for velocity and prioritises time cost for devising minimum time trajectory solutions.

5 Model validation and analysis of results

The model is tested in two stages, i.e., by individually rerouting aircraft trajectories to evaluate their dynamics, and by simulating multiple aircraft trajectories at sector level to validate their traversal through the sector using shifts. For model validation, the limitation in shifts is varied for individual aircraft trajectories to analyse the benefits of these shifts. The air traffic scenarios are solved using CPLEX optimisation software installed on a 3.5 GHz processor having 32 GB RAM, and the results obtained are analysed and plotted using Matlab 2017b.

5.1 Testing the dynamics for individual aircraft

The dynamics of trajectory rerouting formulated in Sect. 4.1 are evaluated by testing the model against artificially generated complex air traffic scenarios. This is done to evaluate turning rates, flight speeds and acceleration for individual aircraft.

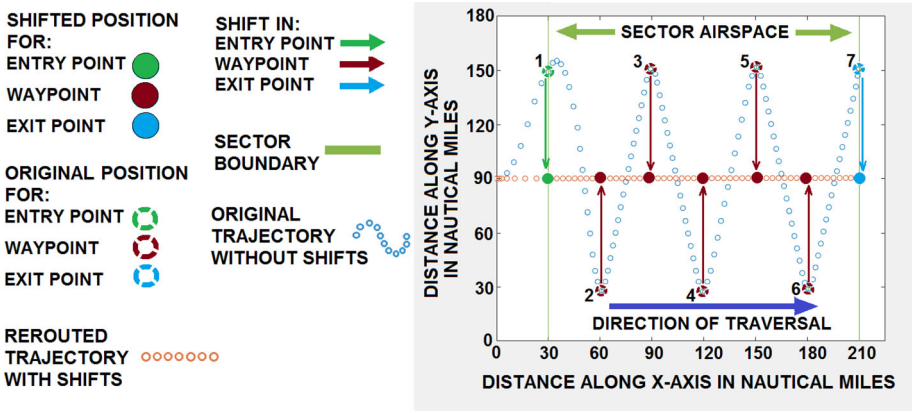

Fig. 9 Single aircraft trajectory rerouting with and without shifts in navigation points. (Color figure online)

By considering the parameters of a commercial aircraft Boeing-747 given by Abdel-Raheem et al. (2019) and Cavcar (2004) for nominal speed $v_{nom} = 259$m/s, minimum flyable speed $v_{min_fly} = 128$m/s, and maximum force $f_{max} = 0.5$N with a point mass of 1kg, and the weights $\alpha = 1$ for cost of time, $\beta = 1$ for cost of velocity and $\gamma = 1$ for cost of force in objective function, the dynamics for a single aircraft are discretised at a time step of 3 s. The value of $R = 40$ is considered for force and velocity constraints in Eqs. (4) and (5), and conflict avoidance constraints in Eq. (8) which gives a small error value of 0.0031% in comparison to the implementation of actual non-linear representation for these constraints.

This aircraft is simulated by the model to visit the waypoints in sequence of time steps, inside the sector for two cases, with and without shifts as shown in Fig. 9. It is seen that the aircraft by using shifts traverses a short and easy path in the form of a straight line, and on the contrary, without using shifts follows a complex zig-zag path with numerous turns. This scenario verifies the successful traversal of aircraft trajectory through sector for both cases and shows the benefits that can be obtained by allowing trajectory deviations. Therefore, it can be said the dynamics formulated in Sect. 4.1 allow the aircraft trajectories to reroute individually through an airspace sector with and without shifts in the navigation points.

Considering the impact of weights in objective function in Eq. (26) on the formulated dynamics, the aircraft is again simulated under the same scenario as shown in Fig. 9 without using shifts. The impact is analysed by varying the value for each weight individually along a certain scale. Figures 10, 11and 12show the different set of trajectories obtained by varying weights of α, β and γ respectively for a range of values on a scale of $0.2 - 8$. The impact of these weights on the trajectories becomes clearer initially due to the horizon effect, but reduces as the horizon effect decreases. This effect occurs as the computer searches limited solution space for rerouting the trajectories, based on the initial parameter values of trajectories that are given as input. This also hinders finding better trajectory solutions.

Figure 10 shows that increasing the value of α which is the weight for time cost, increases sharpness of turns for the aircraft trajectory initially due to the horizon effect. However, increasing the value of β for velocity cost in Fig. 11 and γ for force cost in Fig. 12 decreases the sharpness of turns. It is also observable in these figures that the aircraft trajectory in every case has been able to sequentially visit all the waypoints.

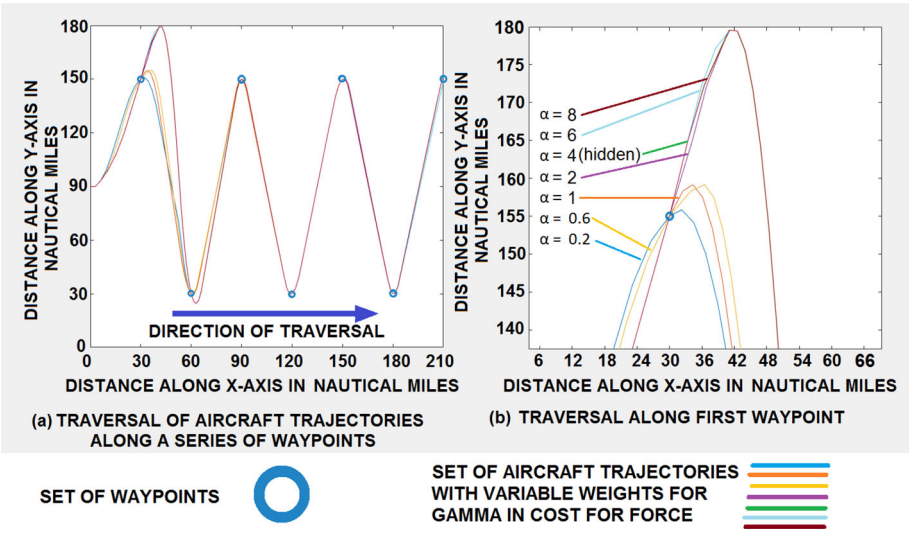

Fig. 10 An illustration of rerouting aircraft trajectory by varying value of alpha α. (Color figure online)

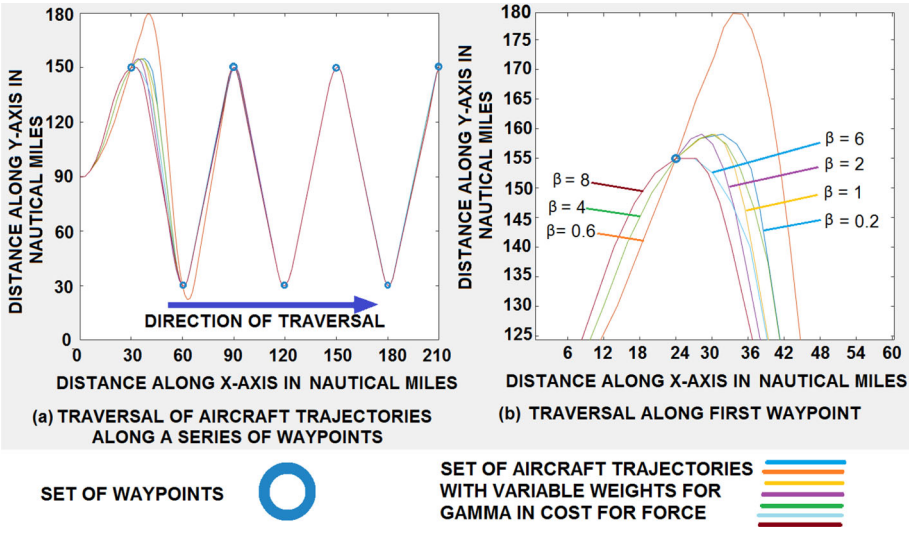

Fig. 11 An illustration of rerouting aircraft trajectory by varying value of beta β. (Color figure online)

5.2 Validating model for multiple aircraft trajectories at an airspace sector level

This section aims to validate the proposed model using the real world data for rerouting multiple aircraft trajectories through an airspace sector, by using shifts in navigation points individually for each trajectory. The results obtained by implementation of these shifts are also analysed at the end of this section.

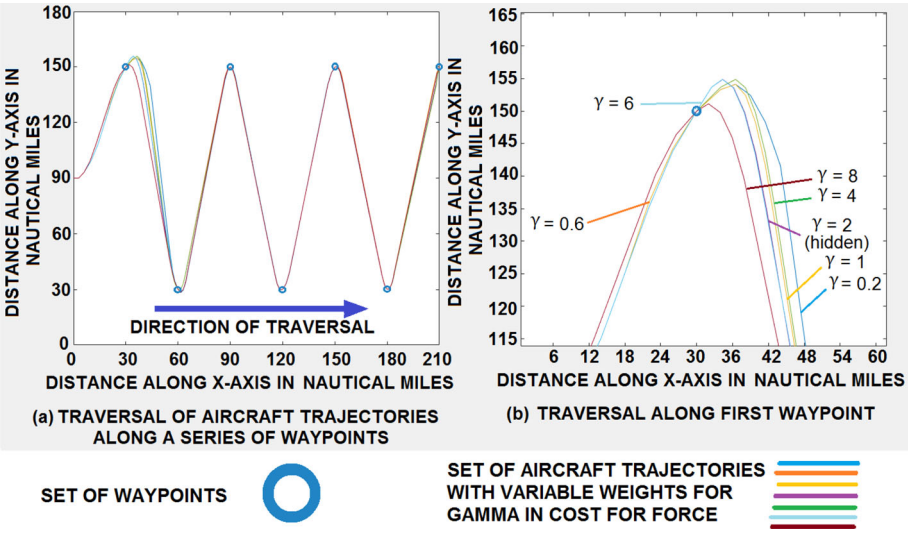

Fig. 12 An illustration of rerouting aircraft trajectory by varying value of gamma γ. (Color figure online)

5.2.1 Using real world data for model validation

Using operational data for real world air traffic and airway structure can help to validate our model by simulating results close to real world conditions, and also allow the readers of this paper to visualise how aircraft trajectories could possibly deviate from the route centreline and get optimised by shifting real world navigation points. However, many previous studies have not considered validating their models against scenarios based on the real world operational data.

We test our model at a time step of 3 s against a series of scenarios derived from operational data of enroute air traffic on the day of 13$^{\text{th}}$October, 2017 from Strumble airspace sector, and consider its actual airway structure at enroute level for shifting navigation points. By using the same parameters mentioned in Sect. 5.1 for v_{nom}, v_{min_fly} and f_{max} with the values of $\alpha = 1$, $\beta = 1$ and $\gamma = 1$, we simulate scenarios by varying limitation of aforementioned shifts on a scale from 0 − 27NM and analyse the impact of this variation on the plots of devised trajectory solutions, and the objective function value for each scenario. The maximum limitation for the pertinent shifts has been chosen to be 27NM as this was the maximum deviation of an aircraft trajectory that we observed in the real world data (see Sect. 3). The air traffic which traversed Strumble on 13^{th} October, 2017 is shown in Fig. 13a which also elaborates how real world aircraft trajectories can possibly deviate from airways while traversing through the sector.

There are certain assumptions that we are required to make for creating scenarios from this operational data. Although most aircraft enter the sector, travel along identifiable airways and exit the sector, some deviate from this. These have been categorised into three different groups and the assumptions made for each group are explained as follows.

1. For the first group of aircraft trajectories shown in the Fig. 13b, it is difficult to find airways being followed by them as they cross many airways and seem to follow the waypoints located on multiple, but closely allocated airways. For this set of trajectories, we consider

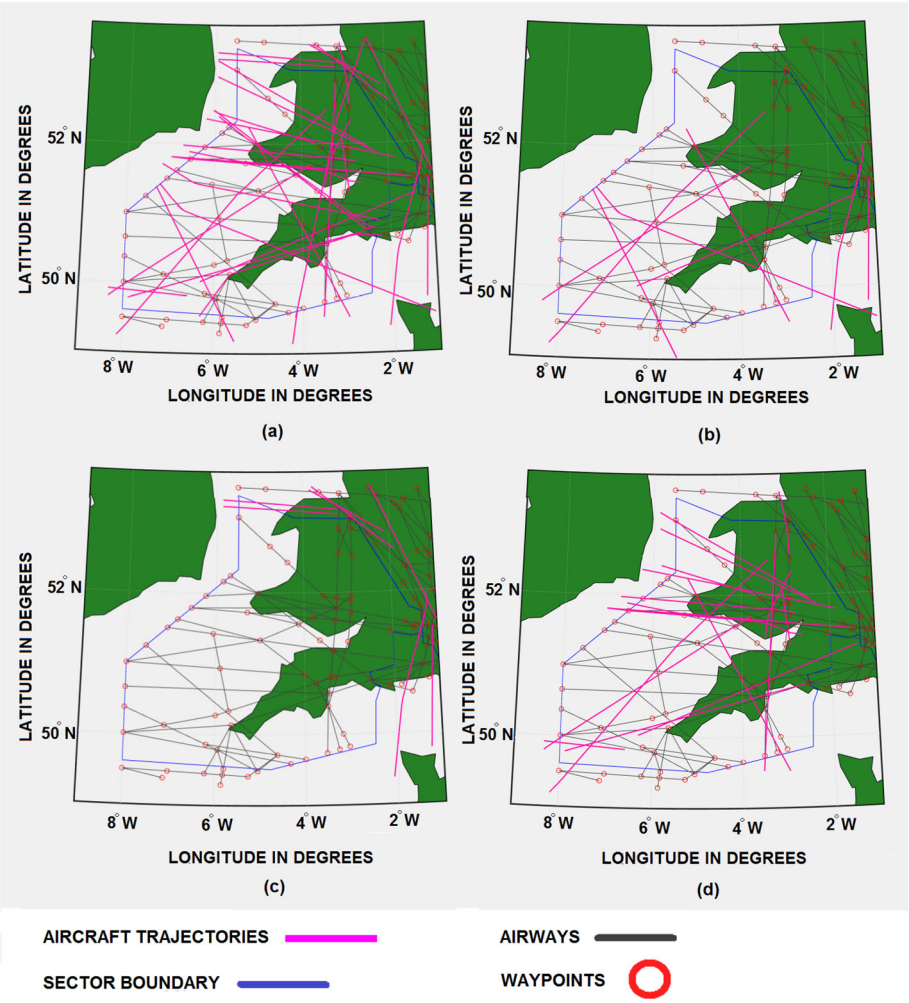

Fig. 13 **a** Complete set of real aircraft trajectories, **b** the trajectories that cross multiple airways in strumble airspace sector, **c** those that fly outside sector boundary and **d** those that disappear and/or initiate within sector boundary. (Color figure online)

the position of navigation points that are located closest to them as an assumption for their original route.

2. For the second group, consisting of a few aircraft trajectories shown in Fig. 13c, it is observed that they fly outside Strumble airspace sector but interact with the trajectories flying inside it, and therefore have been included in the air traffic scenarios for model validation.
3. For the aircraft trajectories belonging to the third group as shown in Fig. 13d, it is seen that they disappear and/or initiate within the sector boundary as their portion lying in enroute airspace is only visible. Therefore, these trajectories are assumed to have fixed entry and exit points at their point of appearance and disappearance inside the sector airspace.

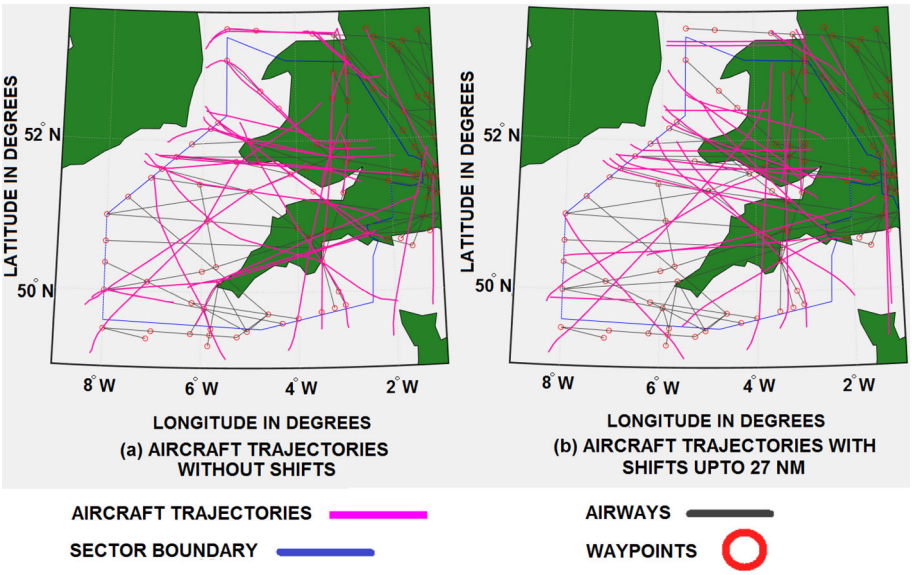

Fig. 14 Comparison of aircraft trajectory solutions with minimum (0NM) and maximum (27NM) limitation for shifts. (Color figure online)

Moreover, the number of entry and exit points located close to every aircraft trajectory for assignment have been considered equal to three.

5.2.2 Obtaining and analysing results

The results are obtained by creating scenarios and varying the limitation for shifts in navigation points for implementing trajectory deviations.

The plots of devised trajectory solutions for all scenarios, with limitation of shifts up to 0NM and 27NM are shown in Fig. 14a and b respectively. It can be clearly seen in Fig. 14a that every aircraft trajectory without the allowance of shifts is forced to reroute through the exact position of its navigation points while avoiding conflicts. Moreover, some aircraft trajectories are forced to traverse in curves while following their path. On the other hand, Fig. 14b shows that all the trajectories have been able to traverse without conflicts by using shifts and are similar to the set of real aircraft trajectories given in Fig. 13a, as both sets of trajectories travel in straight lines. This shows that the devised trajectory solutions obtained using maximum limitation of shifts are close to the real world conditions. Furthermore, the curves found in the trajectories in Fig. 14a are not found in trajectories in Fig. 14b, which shows that the devised trajectory solutions with maximum limitation of shifts are easy to traverse in manoeuvring as well for the pilots.

The speeds of all aircraft trajectories derived using both ways i.e. with and without shifts, were observed to satisfy the lower bound of minimum flyable speed v_{min_fly}, the upper bound of nominal speed v_{nom}. Therefore, the trajectory solutions for both cases were flyable with respect to their speeds. Moreover, the turning rates for both cases of trajectories were also observed to satisfy the limit of nominal turning rate ω_{nom}, which indicates the absence of sharp turns and verifies the ease in manoeuvring for the aircraft trajectories. Hence, the derived trajectory solutions are close to real world conditions.

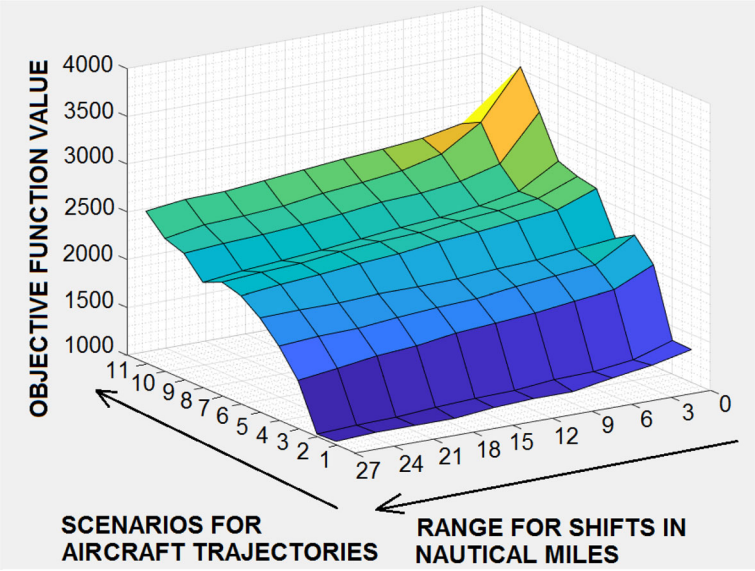

Fig. 15 Impact of varying limitation for shifts in navigation points on the objective function values for air traffic scenarios. (Color figure online)

The impact on objective function values due to the variation in limitation of the shifts is shown in Fig. 15 demonstrates how relaxing constraints to allow larger shifts minimises the objective function value for every scenario, which could possibly help optimise trajectory solutions by reducing their time cost and fuel (velocity and acceleration) cost.

By using shifts up to 27NM, a saving of 4.04 miles (3.52 NM) in total travelling distance and 55.35 s in total travelling time (i.e. 5.47% reduction in time costs) per flight has been calculated, as compared to without using shifts. A Boeing-747 uses 5 gallons or 15.20 kg of fuel per mile (William Roberson & Adams, 2007) and 190 kg of fuel per minute (NATS, 2013) by estimate. By these calculations, saving in total travelling time and distance is quantified to save 236 kg of fuel per flight which as per Flybe estimates in (NATS, 2013) can yield US$ 29.32 million worth annual savings. However, a reduction of 221.05 s in total travelling time and 5.4 miles (4.67 NM) in total travelling distance per flight has also been calculated when the trajectory solutions using maximum limitation for shifts are compared with the real aircraft trajectories, with estimated annual fuel savings of 782 kg fuel savings per flight found using the same calculations (William Roberson & Adams, 2007; NATS, 2013). Therefore, using shifts up to 27NM in trajectories saves fuel and time costs as compared to the trajectories derived without using shifts and, also as compared to the real aircraft trajectories as shown in Fig. 16a and b, which benefits the airlines.

Based on the above analysis, it is clear that increasing the flexibility for shifts in navigation points for allowing trajectory deviations not only allows the aircraft trajectories to perform easy manoeuvring by traversing in straight lines within nominal speed and turning rate, but also reduces fuel and time costs while avoiding conflicts. Adding flexibility to straighten the trajectory should continue to give benefits until the trajectory has reached the optimal, straight path, at which point further flexibility will give no further benefit.

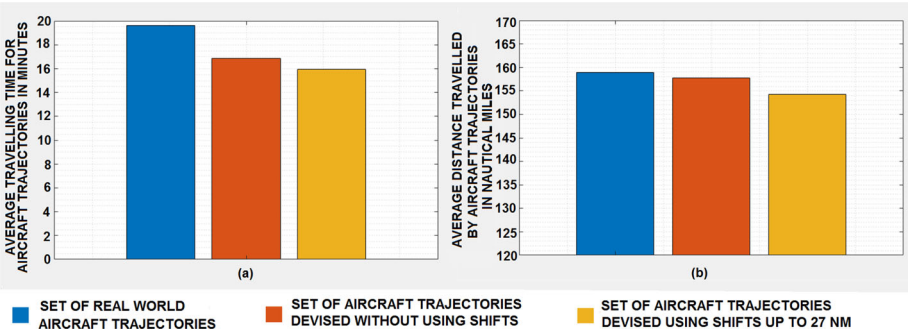

Fig. 16 Comparison of average travelling time and distance by real and devised aircraft trajectories. (Color figure online)

6 Conclusion

This article offline analysed the potential benefits of trajectory deviations, by shifting the navigation points for planar trajectory optimisation at tactical level in an enroute airspace sector. A MILP model was built to allow optimisation of trajectories for aircraft. By analysing real world data for trajectory deviations, the proposed model implemented shifts in navigation points within real world limits to make them manageable in practice by the ATCs. The model was validated using real world data and the aircraft trajectories were optimised in terms of easy manoeuvring, reduced fuel and time costs by allowing limited deviations. Results from the model indicate benefits achievable for major stakeholders of ATM by formulating basic ATC activities at enroute sector level, easing manoeuvres of trajectory rerouting for the pilots and, saving fuel and time costs for the airlines.

Author Contributions Methodology, formal analysis and investigation, and writing-original draft preparation was performed by Salman Arif. All authors contributed to the conceptualisation, data collection, writing-review and editing of this research. All authors read and approved the final manuscript.

Funding This work was funded by the University of Nottingham.

Data availability The data used for the findings of this research is easily available.

Code Availability The code used for the findings of this research is available on request.

Declarations

Conflict of interest The authors declare that they have no known competing financial interests or personal relationships that could have appeared to influence the work reported in this paper.

Consent to participate Not applicable.

Consent for publication Not applicable.

Ethics approval Not applicable.

References

Abdel-Raheem, A. A. M., Hanna, P. A. S., Abdel-Hameed, I. A. M. (2019). Aerodynamic study of boeing airfoil. 4th IUGRC International Undergraduate Research Conference

Adacher, L., Flamini, M., & Romano, E. (2017). Sectors co-operation in air traffic management. *IFAC-PapersOnLine, 50*(1), 4222–4227.

Alam, S., Hossain, M. M., Al-Alawi, F., & Al-Thawadi, F. (2015). Optimizing lateral airway offset for collision risk mitigation using differential evolution. *Air Traffic Control Quarterly, 23*(4), 301–324.

Alonso-Ayuso, A., Escudero, L. F., & Martín-Campo, F. J. (2014). On modeling the air traffic control coordination in the collision avoidance problem by mixed integer linear optimization. *Annals of Operations Research, 222*(1), 89–105.

Archibald, J. K., Hill, J. C., Jepsen, N. A., Stirling, W. C., & Frost, R. L. (2008). A satisficing approach to aircraft conflict resolution. *IEEE Transactions on Systems, Man, and Cybernetics, Part C (Applications and Reviews), 38*(4), 510–521.

Barnier, N., & Brisset, P. (2004). Graph coloring for air traffic flow management. *Annals of Operations Research, 130*(1), 163–178.

Bongiorno, C., Gurtner, G., Lillo, F., Mantegna, R., & Miccichè, S. (2017). Statistical characterization of deviations from planned flight trajectories in air traffic management. *Journal of Air Transport Management, 58*, 152–163.

Carreras-Maide, J., Lordan, O., & Sallan, J. M. (2020). Cost savings from trajectory deviations in the European air space. *Journal of Air Transport Management, 88*, 101887.

Cavcar, M. (2004). Stall speed. Tech rep., Anadolu University, School of Civil Aviation, Turkey, Technical report

Chaimatanan, S., Delahaye, D., & Mongeau, M. (2015). Aircraft 4d trajectories planning under uncertainties. *Computational Intelligence* (pp. 51–58). IEEE Symposium Series on, IEEE.

Chaimatanan, S., Delahaye, D., & Mongeau, M. (2014). A hybrid metaheuristic optimization algorithm for strategic planning of 4d aircraft trajectories at the continental scale. *IEEE Computational Intelligence Magazine, 9*(4), 46–61.

Clarke, L., Johnson, E., Nemhauser, G., & Zhu, Z. (1997). The aircraft rotation problem. *Annals of Operations Research, 69*, 33–46.

Cook, A., Tanner, G., Williams, V., & Meise, G. (2009). Dynamic cost indexing-managing airline delay costs. *Journal of Air Transport Management, 15*(1), 26–35.

Delahaye, D., Puechmorel, S. (2000). Air traffic complexity: Towards intrinsic metrics. *Proceedings of the third USA/Europe Air Traffic Management R & D Seminar*

Eurocontrol (2018). Annual network operations report.

Eurocontrol (2020). Monthly network operations report.

Flener, P., Pearson, J., Ågren, M., Garcia-Avello, C., Celiktin, M., & Dissing, S. (2007). Air-traffic complexity resolution in multi-sector planning. *Journal of Air Transport Management, 13*(6), 323–328.

Frazzoli, E., Mao, Z. H., Oh, J. H., & Feron, E. (2001). Resolution of conflicts involving many aircraft via semidefinite programming. *Journal of Guidance, Control, and Dynamics, 24*(1), 79–86.

Gurtner, G., Bongiorno, C., Ducci, M., & Miccichè, S. (2017). An empirically grounded agent based simulator for the air traffic management in the SESAR scenario. *Journal of Air Transport Management, 59*, 26–43.

Hossain, M. M., Alam, S., Symon, F., & Blom, H. (2014). A complex network approach to analyze the effect of intermediate waypoints on collision risk assessment. *Air Traffic Control Quarterly, 22*(2), 87–114.

Kistan, T., Gardi, A., Sabatini, R., Ramasamy, S., & Batuwangala, E. (2017). An evolutionary outlook of air traffic flow management techniques. *Progress in Aerospace Sciences, 88*, 15–42.

Krozel, J., Penny, S., Prete, J., Mitchell, J. (2004). Comparison of algorithms for synthesizing weather avoidance routes in transition airspace. *AIAA Guidance, Navigation, and Control Conference and Exhibit*, p. 4790.

Krozel, J., Jakobovits, R., & Penny, S. (2006). An algorithmic approach for airspace flow programs. *Air Traffic Control Quarterly, 14*(3), 203–229.

Murrieta Mendoza, A., Botez, R. (2014). Vertical navigation trajectory optimization algorithm for a commercial aircraft. *AIAA/3AF Aircraft Noise and Emissions Reduction Symposium*, p. 3019.

NATS (2013). Ten steps to flight efficiency

Planning ,J. (2008). Development office. next generation air transportation system integrated work plan: A functional outline. Tech. rep., Technical report, Joint Planning and Development Office, Washington, DC.

Qian, X., Mao, J., Chen, C. H., Chen, S., & Yang, C. (2017). Coordinated multi-aircraft 4d trajectories planning considering buffer safety distance and fuel consumption optimization via pure-strategy game. *Transportation Research Part C: Emerging Technologies, 81*, 18–35.

Ren, P., & Li, L. (2018). Characterizing air traffic networks via large-scale aircraft tracking data: A comparison between china and the us networks. *Journal of Air Transport Management, 67*, 181–196.

Richards, A., How, J. P. (2002) Aircraft trajectory planning with collision avoidance using mixed integer linear programming. *Proceedings of the American Control Conference, 2002*. IEEE, vol. 3, pp. 1936–1941.

Schuster, W., & Ochieng, W. (2014). Performance requirements of future trajectory prediction and conflict detection and resolution tools within SESAR and NextGen: Framework for the derivation and discussion. *Journal of Air Transport Management, 35*, 92–101.

SESAR. (2007). *Milestone deliverable d3: The atm target concept*. Technical report.

Soler, M., Zou, B., & Hansen, M. (2014). Flight trajectory design in the presence of contrails: Application of a multiphase mixed-integer optimal control approach. *Transportation Research Part C: Emerging Technologies, 48*, 172–194.

Vela, A., Solak, S., Singhose, W., Clarke, J. P. (2009) *A mixed integer program for flight-level assignment and speed control for conflict resolution*. Decision and Control, 2009 held jointly with the 2009 28th Chinese Control Conference. CDC/CCC 2009. Proceedings of the 48th IEEE Conference on, IEEE, pp. 5219–5226.

Wang, H., Song, Z., & Wen, R. (2018). Modeling air traffic situation complexity with a dynamic weighted network approach. *Journal of Advanced Transportation*. https://doi.org/10.1155/2018/5254289

William Roberson, R. R., Adams, D. (2007). Fuel Conservation Strategies: Cruise Flight

Yang, Y., Prandini, M., Cao, X., & Du, W. (2017). A multi-criteria decision-making scheme for multi-aircraft conflict resolution. *IFAC-PapersOnLine, 50*(1), 14674–14679.